CHAOS AND COMPLEXITY IN A FOUR-DIMENSIONAL SYSTEM WITH HYPERBOLIC TANGENT NONLINEARITY AND NO EQUILIBRIUM

M. I. KOPP^{1*}, §

ABSTRACT. This paper introduces a new four-dimensional (4-D) dynamical system composed of only seven terms: four linear terms, one nonlinear term involving the hyperbolic tangent function, one absolute value function term, and a constant. The new 4-D system does not have any equilibrium points and is capable of producing hidden attractors. The paper includes a detailed dynamical analysis, which encompasses bifurcation diagrams, Lyapunov exponents, Kaplan-Yorke dimensions, and bias amplification. Additionally, the theoretical model is verified through an electronic simulation of the system using Multisim[©] 14.2. The paper also demonstrates the synchronization of two identical 4-D hyperchaotic systems using the active control method. The proposed simple dynamic system exhibits a rather complex chaotic behavior and may find applications in various practical domains.

Keywords: hyperchaotic behavior, offset boosting control, circuit implementation, active control synchronization

AMS Subject Classification: 34Cxx, 34C28

1. Introduction

In recent years, the rapid advancement of chaos theory has led to its widespread application across various engineering fields, including lasers [?], power systems [?], oscillators [?], neural networks [?], cryptosystems [?], memristive systems [?], and more. Lorenz's discovery of a three-dimensional (3D) chaotic system [?] sparked the exploration of various other chaotic systems. The introduction of the first four-dimensional hyperchaotic system by Rössler [?]-[?] marked a turning point, leading to increased scientific interest in hyperchaos, as these nonlinear dynamic systems display more intricate behavior than chaotic systems. A hyperchaotic system is mathematically defined as a chaotic system that possesses more than one positive Lyapunov exponent, resulting in richer and more complex dynamics within the phase plane [?].

¹ Institute for Single Crystals, NAS Ukraine, Nauky Ave. 60, Kharkiv 61072, Ukraine. e-mail: michaelkopp0165@gmail.com; ORCID: https://orcid.org/0000-0001-7457-3272.

^{*} Corresponding author.

[§] Manuscript received: October 16, 2024; accepted: February 26, 2025.

TWMS Journal of Applied and Engineering Mathematics, Vol.15, No.11; © Işık University, Department of Mathematics, 2025; all rights reserved.

Chaotic systems can be classified into two categories: those with self-excited attractors and those with hidden attractors. A self-excited attractor possesses a basin of attraction that intersects with the vicinity of an equilibrium point, while a hidden attractor has a basin of attraction that does not intersect with the neighborhood of any equilibrium point [?]. The idea of hidden attractors, introduced in [?], has inspired ongoing research in the field of nonlinear science. According to the article [?], currently hidden attractors within dynamic systems are divided into five categories: 1) systems without equilibria [?], 2) equilibrium curves [?], 3) planes of curves [?], 4) equilibrium lines [?], and 5) stable equilibrium points [?]. Researchers have focused on constructing new chaotic and hyperchaotic models, taking into account the following aspects: 1) the presence of several positive Lyapunov exponents; 2) minimizing the number of terms in the system; 3) achieving the highest Kaplan-Yorke dimension.

Chaos control and synchronization are significant challenges in chaos theory. The problem of chaos synchronization involves two systems: the master, or driver system, and the slave, or follower system. Various methods have been proposed to address this issue, including active control [?]-[?], adaptive control [?]-[?], backstepping control [?], and sliding mode control [?]-[?], and so on. In this paper, we choose the active control method due to its appealing characteristics, such as rapid convergence and the ease of selecting suitable controllers.

There is an extensive number of 4-D hyperchaotic systems reported in the literature. Therefore, we focus our brief review on 4-D systems with a single nonlinear term but no 4-D chaotic jerk systems. In [?], a 4-D system with eight terms, including a single nonlinear term, was presented, exhibiting different types of hidden attractors. A simple 4-D chaotic system without equilibrium points, displaying hidden attractors with attractor coexistence (multistability), was reported in [?]. This system, also consisting of eight terms with one nonlinear term, exhibits complex behaviors such as 3-torus and 2-torus chaos. In [?], a nonequilibrium autonomous chaotic system was introduced using a linear state feedback controller in the Sprott-S system. The proposed system features eight terms, including a single nonlinear term, and shows complex hidden dynamics, such as hidden multistability. A 4-D system with eight terms and hyperbolic cosine nonlinearity was described in [?]. It is capable of displaying diverse dynamics, including hidden and multiple attractors, and is notable for the simplicity of its electronic analog, which does not require an analog multiplier chip. The system demonstrates behaviors such as chaotic 2-torus and 3-torus. In [?], a 4-D chaotic system incorporating an active flow-controlled memristor with smooth cubic nonlinearity was proposed. This system consists of seven terms, including one nonlinear term, with a Kaplan-Yorke dimension of $D_{KY} = 2.579$. A 4-D chaotic system with a simple structure of 11 terms and a single nonlinear term was presented in [?], featuring a Kaplan-Yorke dimension of $D_{KY} = 3.184$. A simple 4-D chaotic system with hidden attractors was introduced in [?], featuring a hyperbolic cosine function as its nonlinear term. This system exhibits a diverse range of dynamical behaviors, including chaos, quasi-periodicity, and the transition to a 2-torus attractor.

Based on the reviewed literature [?]-[?], no study has yet explored a 4-D hyperchaotic system incorporating a nonlinear term with a hyperbolic tangent function. This gap motivated our investigation of a simple 4-D hyperchaotic system featuring a hyperbolic tangent nonlinearity.

The main contribution for this paper is summarized as follows:

• The proposed system is considered simple, comprising seven terms: four linear terms, one nonlinear term involving the hyperbolic tangent function, one absolute value function term, and a constant.

- A comprehensive dynamical analysis of the 4-D hyperchaotic system is conducted, including the construction of the bifurcation diagram, classification of equilibrium points, and calculation of the Lyapunov exponents and Kaplan-Yorke dimension, as summarized in Table 1.
- An electronic analog of the proposed 4-D system is designed and implemented.
- Active control synchronization of the system is theoretically and numerically demonstrated.

The structure of this paper is organized into five sections as follows. In Section 2, the mathematical model is introduced, and the basic dynamical properties of the new 4-D system with no equilibria are analyzed. In Section 3, the electronic circuit design of the new system is carried out. Active control synchronization is given in Section 4. Finally, Section 5 draws the conclusions of this work.

2. Mathematical model and dynamical analyses of the proposed 4-D system

In this section, we introduce the mathematical formulation of the proposed 4-dimensional hyperchaotic system and perform a detailed dynamical analysis.

2.1. Essential features of the novel 4-D hyperchaotic system. The 4-D system analyzed in the manuscript is a variant of the original chaotic type systems by Rössler in his seminal work [?], and the mathematical expression for the proposed 4-D system takes a relatively simple form:

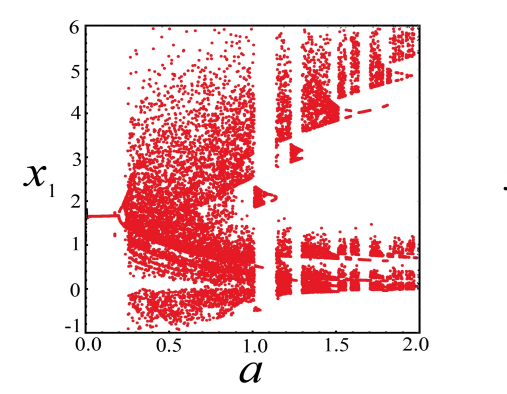
$$\begin{cases} \frac{dx_1}{dt} = a(-x_1 + x_2) + x_4, \\ \frac{dx_2}{dt} = -x_3 \tanh x_1, \\ \frac{dx_3}{dt} = |x_1| - 1, \\ \frac{dx_4}{dt} = -bx_1. \end{cases}$$
(1)

From equation (??), we observe that the system consists of seven terms: a nonlinear term involving the hyperbolic tangent $(x_3 \tanh x_1)$, a term with the absolute value function $(|x_1|)$, a constant term (1), and four linear terms with the state variables x_1, x_2, x_4 . In this system (??), a and b are positive control parameters.

Let's explore the key dynamic properties of the new 4-D system. The system (??) is easily verified to be symmetric with respect to the x_3 -axis and remains invariant under the transformation $(x_1, x_2, x_3, x_4) \rightarrow (-x_1, -x_2, x_3, -x_4)$. To determine the nature of system (??), we calculate its divergence as follows:

$$\frac{\partial \dot{x}_1}{\partial x_1} + \frac{\partial \dot{x}_2}{\partial x_2} + \frac{\partial \dot{x}_3}{\partial x_3} + \frac{\partial \dot{x}_4}{\partial x_4} = -a.$$

It is obvious that the system (??) is dissipative when a > 0. If a < 0, the phase volume expands, and the system (??) becomes unbounded. For a = 0, the system (??) is conservative. Moving forward, we will focus exclusively on the study of the dissipative system (??). To identify the equilibrium points in system (??), we assume $\dot{x}_1 = \dot{x}_2 = \dot{x}_3 = \dot{x}_4 = 0$, which gives us $x_1 = 0$ from the fourth equation. Substituting this into the third equation results in the impossible statement -1 = 0. This logical inconsistency suggests that the system (??) is classified as hidden.



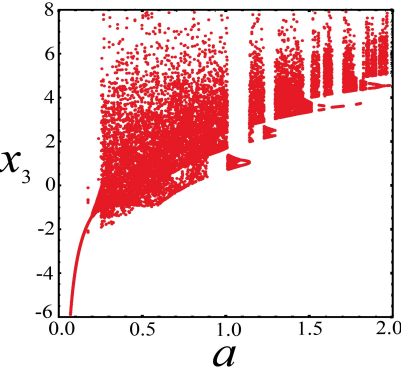


FIGURE 1. Bifurcation diagrams for x_1, x_3 components of the system (??).

2.2. Comprehensive dynamic analysis of the proposed hyperchaotic model. In this subsection, we conduct several analyses to determine whether the proposed system exhibits hyperchaotic behavior. Various dynamic analysis methods will be applied, as they are essential for identifying chaotic or hyperchaotic dynamics in the system.

Let's begin with the bifurcation diagram analysis, a commonly used tool for visually representing changes in the system's state variables. This diagram is crucial for understanding qualitative shifts in the system's behavior as specific control parameters are varied. We solve the system of Eqs. (??) under the initial conditions:

$$x_1(0) = x_2(0) = x_3(0) = x_4(0) = 1.$$
 (2)

The parameter a is varied in system $(\ref{equ:thm.1})$, while the other parameter is kept constant at b=0.55. The bifurcation diagrams in Fig. $\ref{equ:thm.1}$? illustrate the x_1 and x_3 components of system $(\ref{equ:thm.1})$ as a changes within the range $a \in [0,2]$. These diagrams help identify regions of regular behavior within a system, represented by individual points. Regular behavior encompasses predictable, structured, and non-chaotic dynamics. One example is a limit cycle, a stable periodic solution that attracts nearby trajectories. Additionally, regular behavior can include non-periodic motions, such as quasi-periodicity, where the system follows a structured yet non-repeating trajectory. Furthermore, bifurcation diagrams can illustrate period-doubling bifurcations as the parameter a varies. These bifurcations represent a transition where the system shifts from regular periodicity to a doubled period, which may continue progressing and ultimately lead to chaotic behavior.

In-depth insights into the dynamic behavior of the system as parameter a varies can be gained by examining the Lyapunov exponents. The number of Lyapunov exponents corresponds to the dimensionality of the dynamic system. Lyapunov exponents (LEs) quantify the rate at which neighboring trajectories diverge or converge within the system. When an LEs is positive, the dynamic system is deemed unstable or chaotic, while a negative exponent indicates a tendency toward stable equilibrium. Thus, the sign of the LEs facilitates the classification of the system's behavior as regular, quasi-regular (such as 2-torus or 3-torus), chaotic, or hyperchaotic.

All LEs for specific values of parameter a and initial conditions (??) were calculated using the Gram-Schmidt orthonormalization for Benetinn-Wolf's algorithm [?]-[?], which is a standard and reliable approach for determining Lyapunov exponents in dynamical systems. This method (see also [?]) ensures accurate computation of the exponents by iteratively linearizing the system's equations along its trajectory and tracking the divergence of nearby trajectories. As indicated by the Lyapunov exponents, the dynamical

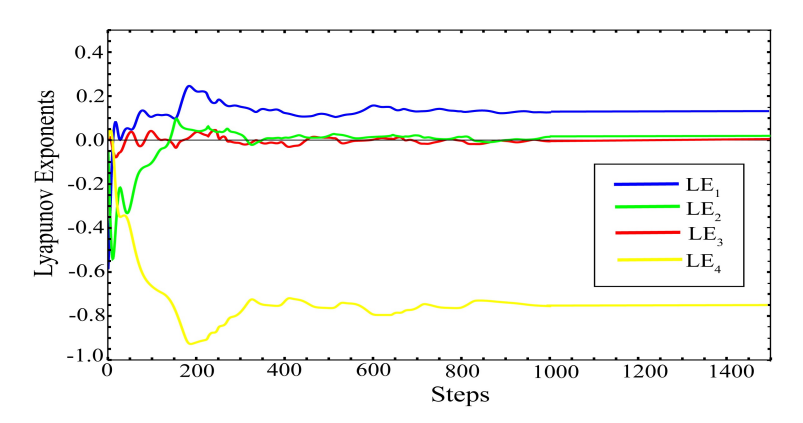


FIGURE 2. Lyapunov exponents for the system (??) for the parameter value a = 0.62 and initial conditions (??).

behaviors of system (??) can be classified into the following categories, as detailed in Table ??. Next, we concentrate on the hyperchaotic behavior of system (??). The pres-

a	Lyapunov Exponents	Signs	Behavior
	(LE_1, LE_2, LE_3, LE_4)		
a = 0.15	(0.0613 , -0.0384, -0.0019, -0.1710)	(0, -, -, -)	Periodic
			(limit cycle)
a = 0.55	(0.1529, 0.0059 , -0.0237, -0.6825)	(+,0,-,-)	Chaotic
a = 0.6	(0.1513, 0.0051 , 0.0035 , -0.7600)	(+,0,0,-)	Chaotic
			2 - torus
a = 0.62	(0.1385, 0.0201, 0.0076 , -0.7864)	(+, +, 0, -)	Hyperchaotic
a = 0.65	(0.0715, 0.0327, -0.0046, -0.7497)	(+, +, 0, -)	Hyperchaotic
a = 0.8	$(0.1463, 0.0055, \mathbf{-0.0049}, -0.9468)$	(+,0,0,-)	Chaotic
			2-torus
a = 1.5	(0.0425, 0.0007 , -0.0463, -1.4969)	(+,0,-,-)	Chaotic

Table 1. Lyapunov exponents for different values of the parameter a.

ence of two positive Lyapunov exponents ((n-2) + positive LEs) confirms that the system exhibits two distinct directions where nearby trajectories diverge exponentially. In this case, the maximum Lyapunov exponent (MLE) is $(LE_1 = 0.138582)$, and the sum of all Lyapunov exponents is negative: $LE_1 + LE_2 + LE_3 + LE_4 = -0.62 < 0$, indicating that the system (??) is dissipative. It can be easily verified that the hyperchaotic system (??) with parameter a = 0.62 satisfies the condition [?]:

$$\sum_{i=1}^{4} LE_i = \sum_{i=1}^{4} \frac{\partial \dot{x}_i}{\partial x_i} = -0.62.$$

The dynamics of Lyapunov exponents associated with hyperchaotic behavior are illustrated in Fig. ??. An estimate of the attractor complexity in the system described by Eq. (1) and with the possibility of giving rise to hyperchaotic dynamics can be obtained by calculating the Lyapunov or Kaplan-Yorke dimension, as explained in [?]:

$$D_{KY} = \xi + \frac{1}{|LE_{\xi+1}|} \sum_{i=1}^{\xi} LE_i = 3 + \frac{0.1664}{0.7864} \approx 3.212,$$
 (3)

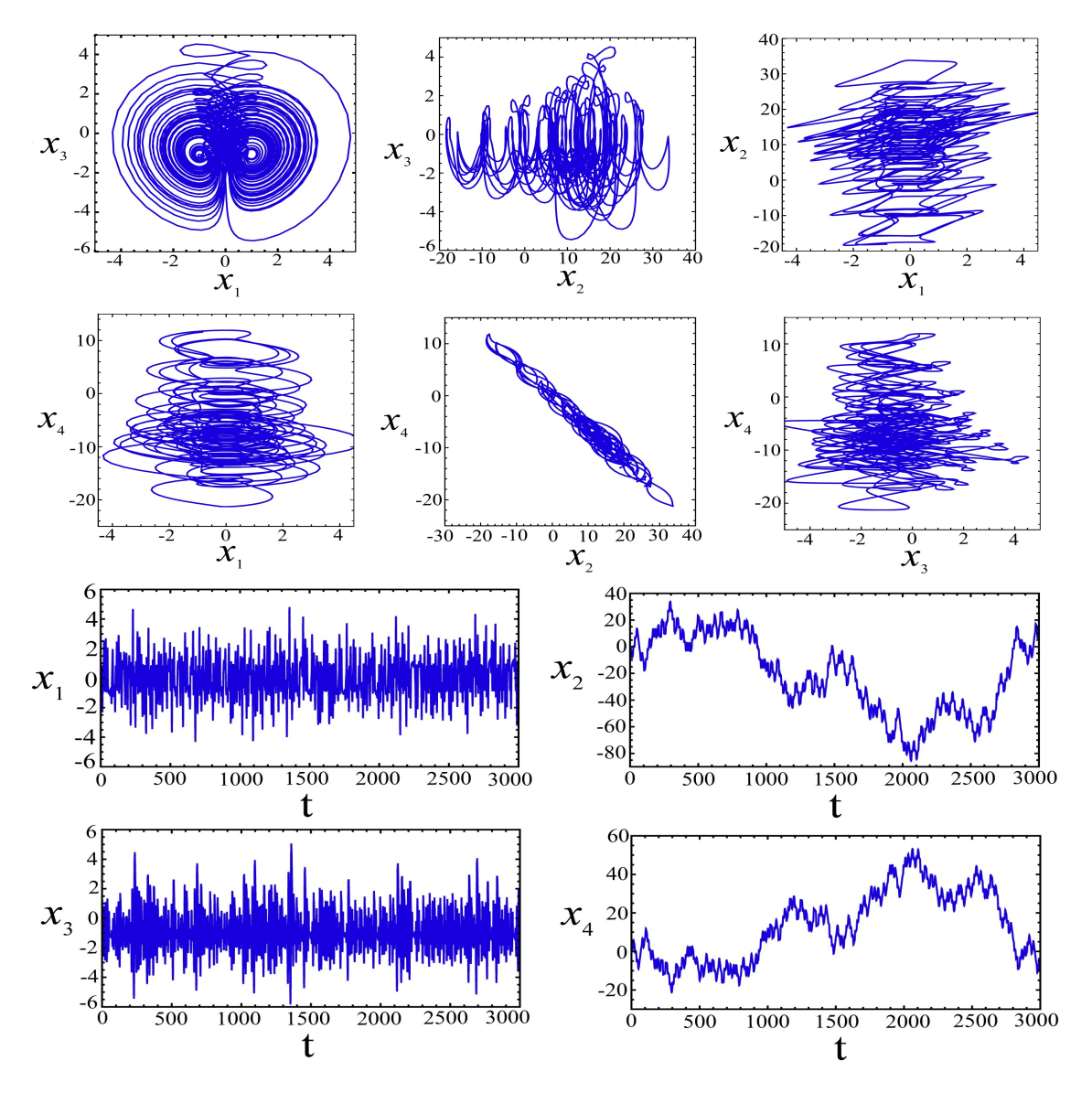


FIGURE 3. Hidden attractors and time diagrams of the new 4-dimensional system (??) with parameters value a = 0.62, b = 0.55, and initial conditions (??).

where ξ is determined from the conditions

$$\sum_{i=1}^{\xi} LE_i > 0 \implies \sum_{i=1}^{3} LE_i = 0.1664, \quad \sum_{i=1}^{\xi+1} LE_i < 0 \implies \sum_{i=1}^{4} LE_i = -0.62 < 0.$$

Here ξ is the number of first non-negative LEs in the spectrum. Dimension D_{KY} (??) is fractional.

2.3. Phase portraits of attractors and offset boosting control. Dynamic systems serve as mathematical models across various scientific disciplines to describe complex phenomena, often exhibiting multiple attractors. These attractors can take the form of points, cycles, tori, or more intricate chaotic structures, representing different potential

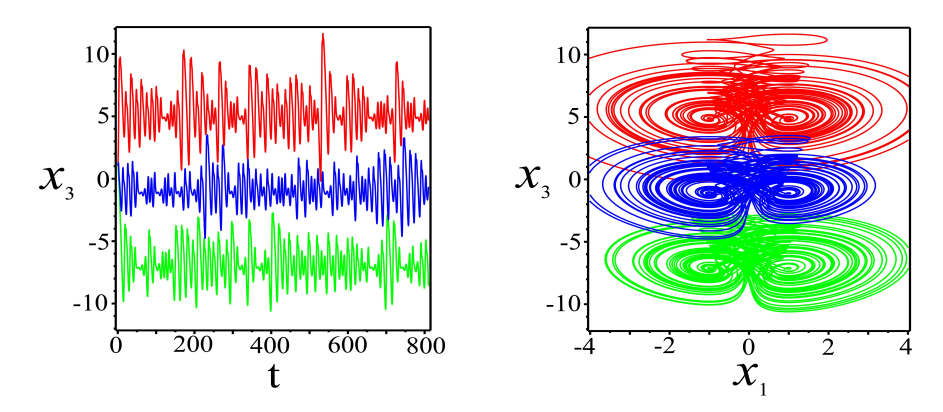


FIGURE 4. Signal x_3 and phase portrait in the plane x_1x_3 for different values of the offset boosting controller k: k = 0 (blue), k = 6 (green), k = -6 (red).

states of the system. As highlighted in the previous subsection, the dynamic system (??) with a=0.62 displays hyperchaotic behavior, making the visual examination of phase portraits of the hyperchaotic attractors particularly intriguing. Using Mathematica[©] 11.1 (hereinafter referred to as Mathematica), we plotted the phase portraits and temporal diagrams of the state components for the hyperchaotic system (??), as shown in Fig. ??. 11.1 Notably, directly implementing the hyperchaotic system (??) in an electronic circuit presents challenges. Fig. ?? illustrates that the dynamic variables x_2 and x_4 operate within a range that exceeds the power supply capabilities of operational amplifiers. This issue is addressed by transforming the variables in the dynamic system (??). Specifically, the scale of the variables is adjusted as follows: $x_2 = 10X_2$ and $x_4 = 10X_4$, while the remaining variables are renamed as $x_1 = X_1$ and $x_3 = X_3$. Then the transformed hyperchaotic system (??) has the form:

$$\begin{cases} \frac{dX_1}{dt} = 0.62(-X_1 + 10X_2) + 10X_4, \\ \frac{dX_2}{dt} = -0.1X_3 \tanh X_1, \\ \frac{dX_3}{dt} = |X_1| - 1, \\ \frac{dX_4}{dt} = -0.055X_1. \end{cases}$$
(4)

In the next section, the transformed system (??) will be employed to develop an analog chaos generator circuit.

The offset boosting control method has numerous applications in hyperchaotic systems, enabling flexible shifting of the attractor in a desired direction through the introduction of an offset, which is highly valuable in engineering contexts [?]. By introducing a constant to specific variables within a system, chaotic signals can be maneuvered throughout the phase space. In the equations of system (??), it is evident that the state variable x_3 appears solely in the second equation. Consequently, we can control these state variables alternately by substituting x_3 with $x_3 + k$ where k is constant. As shown on the left in Fig. ??, modifying the bias gain control k effectively transforms the signal x_3 from a bipolar to a unipolar signal. Adjusting the parameter k shifts the attractor along the x_3 -axis, as illustrated on the right side of Fig. ??.

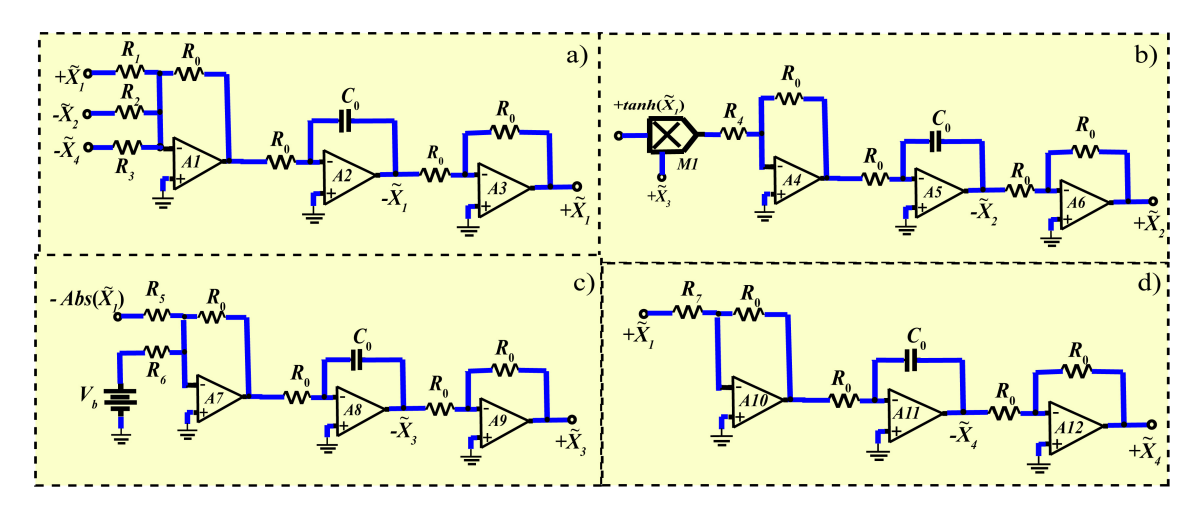


FIGURE 5. Circuit modules implemented based on a system of equations (??): a) \widetilde{X}_1 , b) \widetilde{X}_2 , c) \widetilde{X}_3 , d) \widetilde{X}_4 .

3. Electronic circuit design

In this section, we theoretically model the new hyperchaotic system (??) using Kirchhoff's laws. Following this, we simulate and test the chaos generator's electronic circuit using Multisim[©] 14.2 software. According to Kirchhoff's laws for electrical circuits, the electrical analog of system (??) can be represented as follows:

$$\begin{cases} C_{1} \frac{dU_{1}}{d\tau} = -\frac{U_{1}}{R_{11}} + \frac{U_{2}}{R_{12}} + \frac{U_{4}}{R_{13}}, \\ C_{2} \frac{dU_{2}}{d\tau} = -\frac{U_{3} \tanh(U_{1})}{R_{21} K}, \\ C_{3} \frac{dU_{3}}{d\tau} = \frac{|U_{1}|}{R_{31}} - \frac{\tilde{V}_{b}}{R_{32}}, \\ C_{4} \frac{dU_{4}}{d\tau} = -\frac{U_{1}}{R_{41}}, \end{cases}$$

$$(5)$$

where \widetilde{V}_b is a stable DC voltage source to implement the constant (=1) in a system (??), R_{ij} are resistors $(i,j)=1,2,3,4,5,6,\ U_i(\tau)$ are voltage values, C_i are capacitors, and K is a scaling coefficient for the multiplier. We choose the normalized resistor as $R_0=100\mathrm{k}\Omega$ and the normalized capacitor as $C_0=1\mathrm{nF}$. Then the time constant is equal to $t_0=R_0C_0=10^{-4}\mathrm{s}$. We rescale the state variables of the system (??) as follows $U_1=U_0\widetilde{X}_1, U_2=U_0\widetilde{X}_2, U_3=U_0\widetilde{X}_3, U_4=U_0\widetilde{X}_4, U_5=U_0\widetilde{X}_5, U_6=U_0\widetilde{X}_6, K=U_0K'$, and $\tau=t_0t$. Next, we can write Eqs. (??) in a dimensionless form. After substituting R_0 , $C_1=C_2=C_3=C_4=C_0$, and K'=10 into (??) and comparing the numerical values with the output voltages of the system (??), we obtain the resistor values as follows:

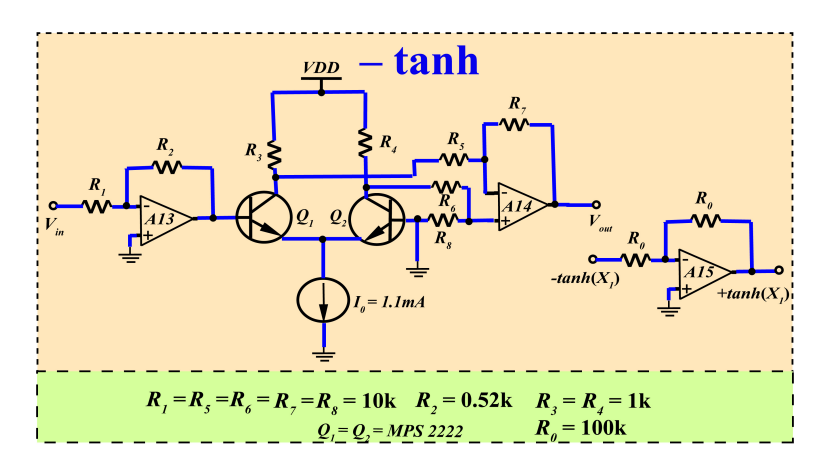


FIGURE 6. Circuit scheme for realization of hyperbolic tangent function.

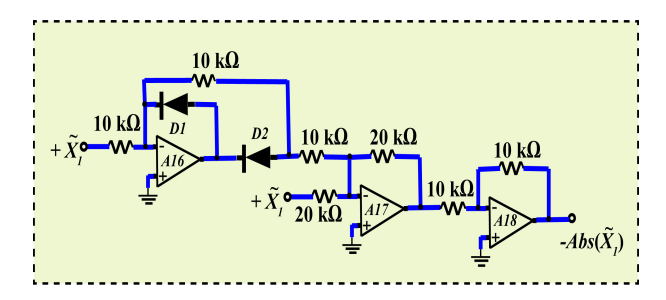


Figure 7. Schematic diagram for the implementation of function absolute value $|\cdot|$.

$$\begin{cases} \frac{d\tilde{X}_{1}}{dt} = -\frac{100k}{R_{1}}\tilde{X}_{1} + \frac{100k}{R_{2}}\tilde{X}_{2} + \frac{100k}{R_{3}}\tilde{X}_{4}, \\ \frac{d\tilde{X}_{2}}{dt} = -\frac{100k}{R_{4} \cdot 10}\tilde{X}_{3} \tanh(\tilde{X}_{1}), \\ \frac{d\tilde{X}_{3}}{dt} = \frac{100k}{R_{5}}|\tilde{X}_{1}| - \frac{100k}{R_{6}}V_{b}, \\ \frac{d\tilde{X}_{4}}{dt} = -\frac{100k}{R_{7}}\tilde{X}_{1}, \end{cases}$$
(6)

where

$$R_1 = 161.29 \text{k}\Omega$$
, $R_2 = 16.129 \text{k}\Omega$, $R_3 = 10 \text{k}\Omega$, $R_4 = R_5 = R_6 = 100 \text{k}\Omega$, $R_7 = 1.818 \text{M}\Omega$.

The analog circuit modules for the equations in system (??) are illustrated in Fig. ??. These circuits consist of standard components, including resistors (R), capacitors (C), diodes D1 and D2 (1N4001), a multiplier (M1, AD633), operational amplifiers (A1-A18, TL084ACN), and a supply voltage of ± 15 V. The constant value of 1 is implemented using a constant voltage source $V_b = 1V$. The electronic circuit designed to implement the hyperbolic tangent function is commonly utilized in studies related to the dynamics of memristive Hopfield neural networks (see, for example, [?]). As shown in Fig. ??, the equivalent circuit for the inverting hyperbolic tangent function consists of two MPS2222 transistors (Q1 and Q2), two TL084ACN operational amplifiers, a current source of $I_0 = 1.1$ mA, and several resistors. The operational amplifiers facilitate subtraction and input

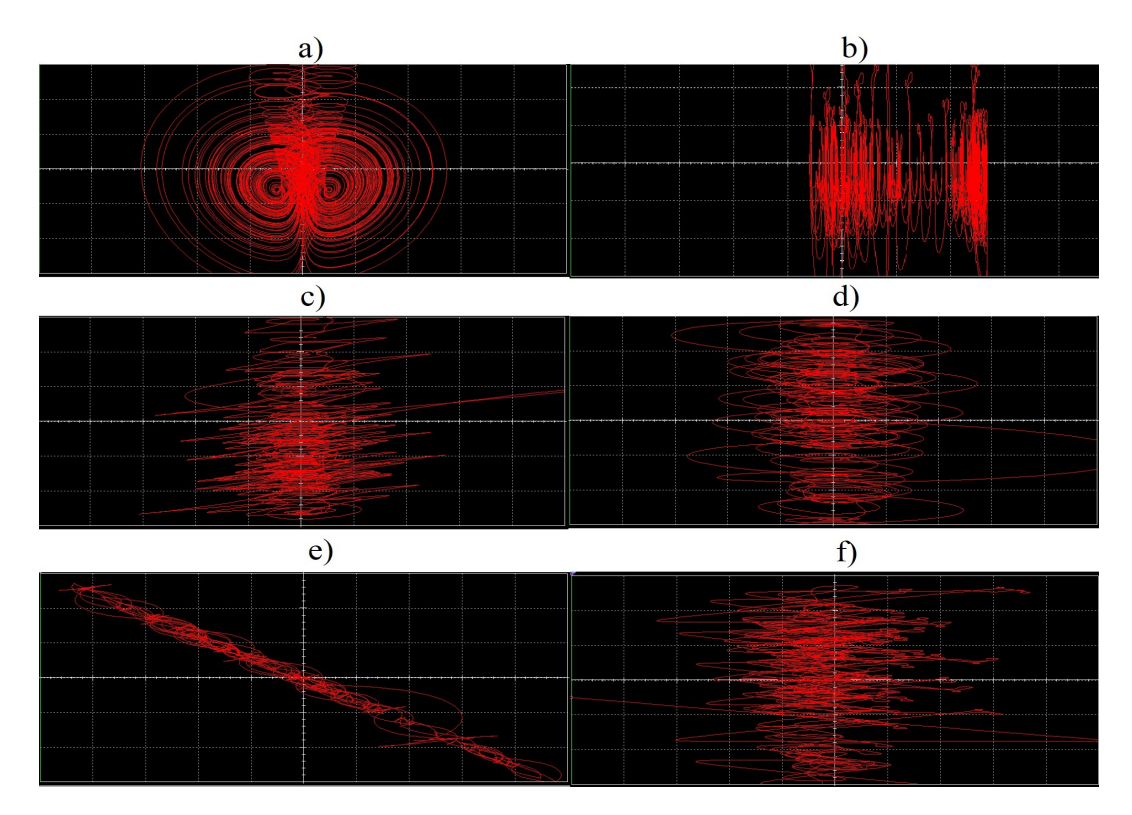


FIGURE 8. Phase portraits of the 4-D hyperchaotic system as generated in Multisim oscilloscopes: a) $\widetilde{X}_1\widetilde{X}_3$, b) $\widetilde{X}_2\widetilde{X}_3$, c) $\widetilde{X}_1\widetilde{X}_2$, d) $\widetilde{X}_1\widetilde{X}_4$, e) $\widetilde{X}_2\widetilde{X}_4$, f) $\widetilde{X}_3\widetilde{X}_4$.

inversion, while the transistors are used to implement the exponential operation. We utilize a standard electronic circuit to model the absolute value function $|\cdot|[?]$, as illustrated in Fig. ?? demonstrate a striking resemblance between the results obtained from Mathematica simulations (Fig. ??) and those from Multisim simulations (Fig. ??).

4. ACTIVE CONTROL SYNCHRONIZATION

The development of a new chaotic oscillator using 4-D nonlinear dynamic equations necessitates an investigation into its synchronization capabilities to confirm practical applicability. In this section, we focus on the active control synchronization [?]-[?] of two identical 4-D hyperchaotic systems. System (??) is chosen as the driver system, and the follower system is outlined as follows:

$$\begin{cases}
\frac{dy_1}{dt} = a(-y_1 + y_2) + y_4 + u_1, \\
\frac{dy_2}{dt} = -y_3 \tanh y_1 + u_2, \\
\frac{dy_3}{dt} = |y_1| - 1 + u_3, \\
\frac{dy_4}{dt} = -by_1 + u_4.
\end{cases}$$
(7)

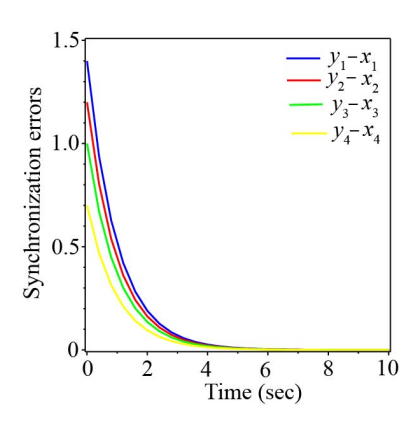


FIGURE 9. Synchronization error behavior for 4-D hyperchaotic driver and follower systems.

In this system, y_1, y_2, y_3, y_4 represent the states, and u_1, u_2, u_3, u_4 are active controllers that will be defined later. The objective is to synchronize the driver and follower systems' signals, even when their initial conditions differ. The state errors are defined as $e_i(t) = y_i(t) - x_i(t)$, for (i = 1, 2, 3, 4). Subtracting the driver system (??) from the follower system (??) gives us the error system as follows:

$$\begin{cases} \dot{e}_{1} = a(-e_{1} + e_{2}) + e_{4} + u_{1}, \\ \dot{e}_{2} = -(y_{3} \tanh y_{1} - x_{3} \tanh x_{1}) + u_{2}, \\ \dot{e}_{3} = |y_{1}| - |x_{1}| + u_{3}, \\ \dot{e}_{4} = -be_{1} + u_{4}. \end{cases}$$
(8)

The next step is to establish active control functions that will generate an asymptotically stable error system, thereby enabling synchronization of the 4-D hyperchaotic systems. The following are the active control functions selected:

$$\begin{cases}
 u_1 = -e_1 + ae_1 - ae_2 - e_4, \\
 u_2 = -e_2 + y_3 \tanh y_1 - x_3 \tanh x_1, \\
 u_3 = -e_3 - (|y_1| - |x_1|), \\
 u_4 = -e_4 + be_1.
\end{cases} \tag{9}$$

Next, the dynamic equations of the error system are given as follows:

$$\begin{cases} \dot{e}_1 = -e_1, \\ \dot{e}_2 = -e_2, \\ \dot{e}_3 = -e_3, \\ \dot{e}_4 = -e_4. \end{cases}$$
(10)

When the proposed active control functions (??) are applied, the error system converts into a linear form. For clarity, this is expressed in matrix form as follows:

$$\begin{vmatrix} \dot{e}_1 \\ \dot{e}_2 \\ \dot{e}_3 \\ \dot{e}_4 \end{vmatrix} = \begin{vmatrix} -1 & 0 & 0 & 0 \\ 0 & -1 & 0 & 0 \\ 0 & 0 & -1 & 0 \\ 0 & 0 & 0 & -1 \end{vmatrix} \begin{vmatrix} e_1 \\ e_2 \\ e_3 \\ e_4 \end{vmatrix}$$
 (11)

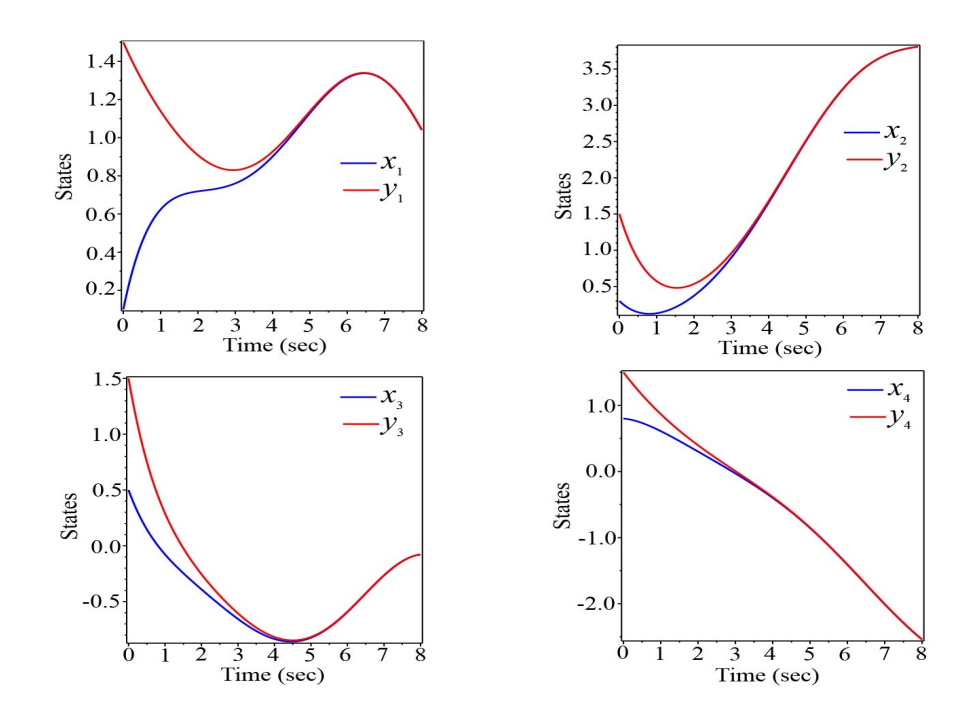


FIGURE 10. Synchronization of the states for 4-D hyperchaotic driver and follower systems.

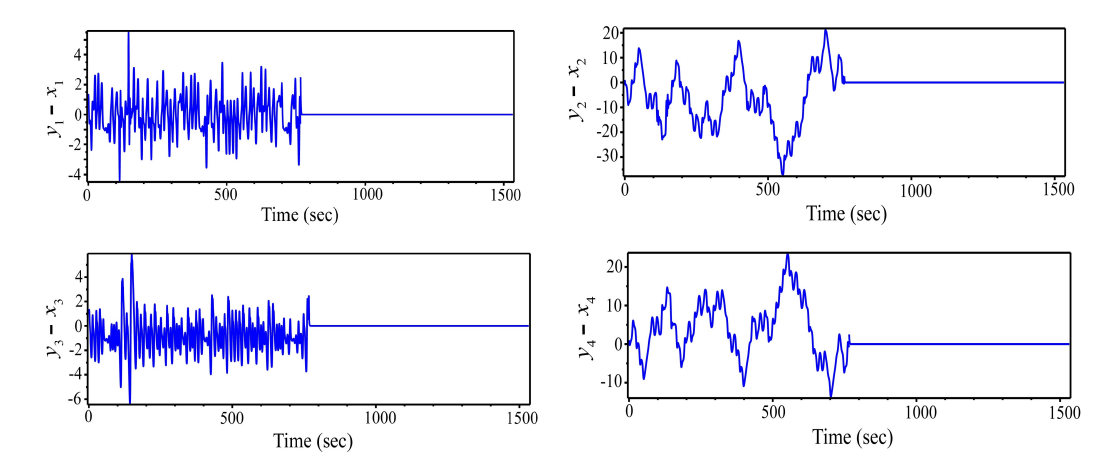


FIGURE 11. Time evolution of the synchronization errors with controllers deactivated (t < 760 s) and activated (t > 760 s).

A simple verification shows that all eigenvalues of the state matrix (??) are negative. Thus, according to the Routh-Hurwitz criterion, the error system is stable, ensuring synchronization between the driver system (??) and the follower system (??).

4.1. **Numerical simulation.** For numerical verification sinchronization, we solved the nonlinear equations (??) and (??) using the 4th-5th order Runge-Kutta-Fehlberg (rkf45) method within the Maple[©] 18 computing environment, with parameters set to a = 0.62 and b = 0.55. The initial conditions for the driver system (??) were as follows:

$$x_1(0) = 0.1, \ x_2(0) = 0.3, \ x_3(0) = 0.5, \ x_4(0) = 0.6,$$
 (12)

and the follower system was initialized with:

$$y_1(0) = y_2(0) = y_3(0) = y_4(0) = 1.5.$$
 (13)

The error curves in Fig. ?? illustrate the synchronization process between the driver and follower systems, with synchronization errors e_i exponentially converging to zero over time. Fig. ?? further depicts the state behaviors in both systems, showing quick trajectory convergence and indicating successful synchronization of the hyperchaotic systems.

To better visualize synchronization using the active control method, we selected a relatively large delay time of t = 760 seconds and set the initial conditions for the driver system (??) and follower system (??) as follows:

$$X_1(0) = X_2(0) = X_3(0) = X_4(0) = 1,$$
 (14)

$$Y_1(0) = Y_2(0) = Y_3(0) = Y_4(0) = 3.5.$$
 (15)

The active controllers were turned on at t=760 seconds, and Fig. ?? illustrates the time evolution of the error states. The simulation results indicate that when the active controllers were off (t<760 s), the synchronization error for the four states exhibited chaotic behavior, signifying the absence of synchronization. Once the controllers were activated (t>760 s), all synchronization error states quickly converged to zero. This behavior can be explained by the stability property of the chosen synchronization scheme. In particular, if the error dynamics (??) are governed by stability criteria, such as the Lyapunov stability theorem or the Routh-Hurwitz asymptotic stability criterion, then the system naturally reduces synchronization errors to zero. Note that the impact of initial conditions depends on the type of synchronization being studied. In our case, with full or exponential synchronization, the system exhibits global stability. As a result, synchronization errors converge to zero across a broad range of initial conditions.

These simulation results demonstrate the effectiveness of the active controllers (??) in synchronizing two identical 4-D hyperchaotic systems, even when starting from different initial conditions.

5. Conclusions

In this paper, we introduce a new 4-D dynamical system that satisfies the fundamental criteria for hyperchaos generation. According to [?], a hyperchaotic system must: (a) be dissipative, (b) have a four-dimensional phase space, and (c) contain at least one nonlinear term. It was determined that the new 4-D dynamic system has no equilibrium points, which may lead to the formation of hidden attractors. We found two positive Lyapunov exponents, and the new 4-D system is recognized as hyperchaotic; its Kaplan-Yorke dimension ($D_{KY} = 3.212$) underscores its intricate nature. The simulation results from the electronic circuit of the proposed 4-D system, designed in Multisim 14, are in good agreement with the results obtained in Mathematica. By developing an appropriate controller using a nonlinear control strategy and analytical linearization, synchronization was achieved between two identical 4-D hyperchaotic systems.

The new system shows great potential for applications in encrypting and decrypting information.

Acknowledgement. I thank anonymous reviewer for valuable suggestions and comments.

References

- [1] Mengue, A. D., Essebe, D. E., Essimbi, B. Z., (2024), High-dimensional hyperchaos and its control in a modified laser system subjected to optical injection, Opt. Quant. Electron., 56, pp. 1101.
- [2] Hunaish, A. S., Tahir, F. R., Abbood, H. A., (2021), Hyperchaos from DTC Induction Motor Drive System, IFAC-PapersOnLine, 54, pp. 81-86.
- [3] Shvets, A., Sirenko, V., (2019), Hyperchaos in Oscillating Systems with Limited Excitation, Springer Proceedings in Complexity, Springer, Cham, pp. 265-273.
- [4] Lin, H., Wang, C., Cui, L., et al., (2022), Hyperchaotic memristive ring neural network and application in medical image encryption, Nonlinear Dyn., 110, pp. 841-855.
- [5] Shahna, K. U., (2023), Novel chaos based cryptosystem using four-dimensional hyper chaotic map with efficient permutation and substitution techniques, Chaos, Solitons & Fractals, 170, pp. 113383.
- [6] Zhou, X., Sun, K., Wang, H., et al., (2024), Coexisting hyperchaos and multistability in a discrete memristor-coupled bi-neuron model, Nonlinear Dyn., 112, pp. 9547-9561.
- [7] Lorenz, E. N., (1963), Deterministic nonperiodic flow, J. Atmos. Sci., 20(2), pp. 130-141.
- [8] Rössler, O. E., (1976), An equation for continuous chaos, Phys. Lett. A, 57(5), pp. 397-398.
- [9] Rössler, O. E., (1979), Continuous Chaos Four Prototype Equations, Ann. NY Acad. Sci., 316, pp. 376-392.
- [10] Sprott, J. C., (2023), Elegant Automation, WORLD SCIENTIFIC, 348 p.
- [11] Leonov, G. A., Kuznetsov, N. V. and Mokaev, T. N., (2015), Homoclinic orbits, and self-excited and hidden attractors in a Lorenz-like system describing convective fluid motion, Eur. Phys. J. Special Topics, 224, pp. 1421-1458.
- [12] Leonov, G. A., Kuznetsov, N. V. Vagaitsev, V. I., (2011), Localization of hidden Chia's attractors, Phys. Lett. A, 375(23), pp. 2230-2233.
- [13] Al-Azzawi, S. F., Hasan, A. M., (2024), A New 4D Hidden Hyperchaotic System with Higher Largest Lyapunov exponent and its Synchronization, Int. J. Math. Comput. Sci., 2, pp. 63-74.
- [14] Zhang, S., Zeng, Y., (2019), A simple Jerk-like system without equilibrium: Asymmetric coexisting hidden attractors, bursting oscillation and double full Feigenbaum remerging trees, Chaos, Solitons & Fractals, 120, pp. 25-40.
- [15] Zhu, X., Du, W. S., (2019), A new family of chaotic systems with different closed curve equilibrium, Mathematics, 7(1), pp. 94.
- [16] Bayani, A., Rajagopal, K., Khalaf, A. J. M., Jafari, S., Leutcho, G. D. and Kengne, J., (2019), Dynamical analysis of a new multistable chaotic system with hidden attractor: Antimonotonicity, coexisting multiple attractors, and offset boosting, Phys. Lett. A, 383, pp. 1450-1456.
- [17] Nazarimehr, F., Rajagopal, K., Kengne, J., Jafari, S. and Pham, V. T., (2018), A new four-dimensional system containing chaotic or hyper-chaotic attractors with no equilibrium, a line of equilibria and unstable equilibria, Chaos, Solitons & Fractals, 111, pp. 108-118.
- [18] Deng, Q., Wang, C., and Yang, L., (2020), Four-wing hidden attractors with one stable equilibrium point, Int. J. Bifurc. Chaos, 30, pp. 2050086.
- [19] Jung, W., Elliot, S. J., and Cheer, J., (2019), Local active control of road noise inside a vehicle, Mech. Syst. Signal Process., 121, pp. 144-157.
- [20] Bhat, M. A. and Shikha, (2019), Complete synchronisation of non-identical fractional order hyper-chaotic systems using active control, International Journal of Automation and Control, 13, pp. 140-157.
- [21] Zhang, H., Zhang, W., Zhao, Y. and Ji, M., (2020), Adaptive state observers for incrementally quadratic nonlinear systems with application to chaos synchronization, Circuits Syst. Signal Process., 39, pp. 1290-1306.
- [22] Tohidi, S., Yildiz, Y. and Kolmanovsky, I., (2020), Adaptive control allocation for constrained systems, Automatica, 121, pp. 1-11.
- [23] Vaidyanathan, S., Volos, C. K. and Pham, V. T., (2014), Hyperchaos, adaptive control and synchronization of a novel 5-D hyperchaotic system with three positive Lyapunov exponents and its SPICE implementation, Arch. Control Sci., 24, pp. 409-446.
- [24] Vaidyanathan, S. and Volos, C. K., (2015), Analysis and adaptive control of a novel 3-D conservative no-equilibrium chaotic system, Arch. Control Sci., 25, pp. 333-353.
- [25] Chu, J. and Hu, W. W., (2016), Control chaos for permanent magnet synchronous motor base on adaptive backstepping of error compensation, Int. J. Autom. Comput., 9, pp. 163-174.
- [26] Rajagopal, K., Guessas, L., Vaidyanathan, S., Karthikeyan, A. and Srinivasan, A., (2017), Dynamical analysis and FPGA implementation of a novel hyperchaotic system and its synchronization using

- adaptive sliding mode control and genetically optimized PID control, Math. Probl. Eng., 2017, pp. 1-14.
- [27] Rajagopal, K., Laarem, G., Karthikeyan, A. and Srinivasan, A., (2017), FPGA implementation of adaptive sliding mode control and genetically optimized PID control for fractional-order induction motor system with uncertain load, Adv. Differ. Equ., 2017, pp. 1-20.
- [28] Yousefpour, A., Hosseinloo, A. H., Yazdi, M. R. H. and Bahrami, A., (2020), Disturbance observer-based terminal sliding mode control for effective performance of a nonlinear vibration energy harvester, J. Intell. Mater. Syst. Struct., 31, pp. 1495-1510.
- [29] Singh, J. P., Roy, B., (2017), Coexistence of asymmetric hidden chaotic attractors in a new simple 4-D chaotic system with curve of equilibria, Optik, 145, pp. 209-217.
- [30] Singh, J. P. and Roy, B. K., (2018), Multistability and hidden chaotic attractors in a new simple 4-D chaotic system with chaotic 2-torus behavior, Int. J. Dyn. Contr., 6(2), pp. 529-538.
- [31] Zhang, S., Zeng, Y., Li, Z., Wang, M., Zhang, X. and Chang, D., (2018), A novel simple no-equilibrium chaotic system with complex hidden dynamics, Int. J. Dyn. Contr., 6(4), pp. 1465-1476.
- [32] Signing, V., Kengne, J., (2018), Coexistence of hidden attractors, 2-torus and 3-torus in a new simple 4-D chaotic system with hyperbolic cosine nonlinearity, Int. J. Dyn. Control, 6, pp. 1421-1428.
- [33] Sahin, M. E., Cam Taskiran, Z. G., Guler, H., Hamamci, S. E., (2020), Application and modeling of a novel 4D memristive chaotic system for communication systems, Circuits Syst. Signal Process., 39, pp. 3320-3349.
- [34] Bouteraa, Y., Mostafaee, J., Kchaou, M., Abbassi, R., Jerbi, H., Mobayen, S., (2022), A New Simple Chaotic System with One Nonlinear Term, Mathematics, 10, pp. 4374.
- [35] Folifack Signing, V.R., Kengne, J., Pone, J.R.M., (2019), Antimonotonicity, chaos, quasi-periodicity and coexistence of hidden attractors in a new simple 4-D chaotic system with hyperbolic cosine nonlinearity, Chaos Soliton. Fract., 118, pp. 187-198.
- [36] Benettin, G., Galgani, L., Giorgilli, A. et al., (1980), Lyapunov Characteristic Exponents for Smooth Dynamical Systems and for Hamiltonian Systems: A Method for Computing All of Them, Meccanica, 15, pp. 9-20.
- [37] Wolf, A., Swift, J. B., Swinney, H. L., and Vastano, J. A., (1985), Determining Lyapunov Exponents from a Time Series, Physica D, 16, pp.285-317.
- [38] Sandri, M., (1996), Numerical Calculation of Lyapunov Exponents, The Mathematica Journal, 6, pp. 78-84.
- [39] Singh, J. P. and Roy, B. K., (2016), The nature of Lyapunov exponents is (+, +, -, -). Is it a hyperchaotic system?, Chaos, Solitons & Fractals, 92, pp. 73-85.
- [40] Frederickson, P., Kaplan, J. L., Yorke, E. D., Yorke, J. A., (1983), The Liapunov Dimension of Strange Attractors, Journal of differential equations, 49, pp. 185-207.
- [41] Wen, J., Feng, Y., Tao, X. and Cao, Y., (2021), Dynamical Analysis of a New Chaotic System: Hidden Attractor, Coexisting-Attractors, Offset Boosting, and DSP Realization, IEEE Access, 9, pp. 167920-167927.
- [42] Deng, Q., Wang, C., Lin, H., (2024), Memristive Hopfield neural network dynamics with heterogeneous activation functions and its application, Chaos, Solitons & Fractals, 178, pp. 114387.
- [43] Sedra, A. S. and Smith, K. C., (1998), Microelectronics Circuits, 4th ed. New York Oxford University Press.
- [44] Wang, X. and Wang, M., (2008), A hyperchaos generated from Lorenz system, Phys. A: Stat. Mech. Appl., 387, pp. 3751-3758.



Michael I. Kopp received Ph.D. degrees in plasma physics and chemistry from the School of Physics and Technology, Kharkiv State University, in 1992. He is working as a senior researcher at the Department of the Theory of Condensed Matter, Institute for Single Crystals, NAS of Ukraine, Kharkiv. He is interested in nonlinear dynamics, chaos theory, fractals, and nonlinear physics.